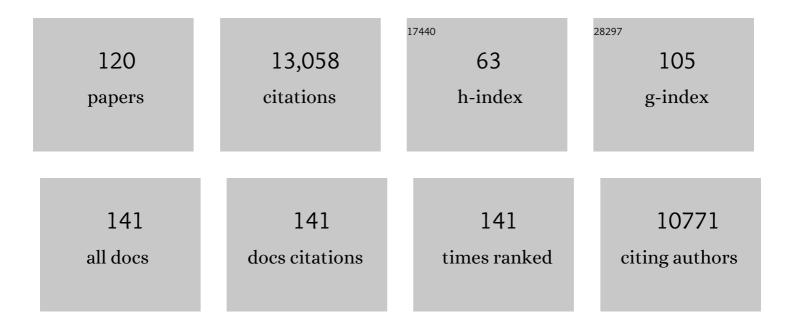
Roland Beckmann

List of Publications by Year in descending order

Source: https://exaly.com/author-pdf/9236153/publications.pdf Version: 2024-02-01



POLAND RECKMANN

#	Article	IF	CITATIONS
1	Inhibition of SRP-dependent protein secretion by the bacterial alarmone (p)ppGpp. Nature Communications, 2022, 13, 1069.	12.8	16
2	Ribosome collisions induce mRNA cleavage and ribosome rescue in bacteria. Nature, 2022, 603, 503-508.	27.8	50
3	Emergence of the primordial pre-60S from the 90S pre-ribosome. Cell Reports, 2022, 39, 110640.	6.4	17
4	Structure of the Maturing 90S Pre-ribosome in Association with the RNA Exosome. Molecular Cell, 2021, 81, 293-303.e4.	9.7	36
5	SAP domain forms a flexible part of DNA aperture in Ku70/80. FEBS Journal, 2021, 288, 4382-4393.	4.7	13
6	Structure of Gcn1 bound to stalled and colliding 80S ribosomes. Proceedings of the National Academy of Sciences of the United States of America, 2021, 118, .	7.1	79
7	The SARSâ€unique domain (SUD) of SARSâ€CoV and SARSâ€CoVâ€2 interacts with human Paip1 to enhance viral RNA translation. EMBO Journal, 2021, 40, e102277.	7.8	26
8	A distinct assembly pathway of the human 39S late pre-mitoribosome. Nature Communications, 2021, 12, 4544.	12.8	27
9	Structural basis of <scp>l</scp> -tryptophan-dependent inhibition of release factor 2 by the TnaC arrest peptide. Nucleic Acids Research, 2021, 49, 9539-9547.	14.5	12
10	A structural inventory of native ribosomal ABCE1â€43S preâ€initiation complexes. EMBO Journal, 2021, 40, e105179.	7.8	35
11	Architecture of the active postâ€ŧranslational Sec translocon. EMBO Journal, 2021, 40, e105643.	7.8	33
12	Molecular mechanism of translational stalling by inhibitory codon combinations and poly(A) tracts. EMBO Journal, 2020, 39, e103365.	7.8	113
13	Structure and function of yeast Lso2 and human CCDC124 bound to hibernating ribosomes. PLoS Biology, 2020, 18, e3000780.	5.6	56
14	Construction of the Central Protuberance and L1 Stalk during 60S Subunit Biogenesis. Molecular Cell, 2020, 79, 615-628.e5.	9.7	48
15	Structural basis for translational shutdown and immune evasion by the Nsp1 protein of SARS-CoV-2. Science, 2020, 369, 1249-1255.	12.6	635
16	Structural basis for the final steps of human 40S ribosome maturation. Nature, 2020, 587, 683-687.	27.8	52
17	90 <i>S</i> pre-ribosome transformation into the primordial 40 <i>S</i> subunit. Science, 2020, 369, 1470-1476.	12.6	59
18	RQT complex dissociates ribosomes collided on endogenous RQC substrate SDD1. Nature Structural and Molecular Biology, 2020, 27, 323-332.	8.2	97

#	Article	IF	CITATIONS
19	Molecular analysis of the ribosome recycling factor <scp>ABCE</scp> 1 bound to the 30S postâ€splitting complex. EMBO Journal, 2020, 39, e103788.	7.8	24
20	Tetracenomycin X inhibits translation by binding within the ribosomal exit tunnel. Nature Chemical Biology, 2020, 16, 1071-1077.	8.0	43
21	Structure of the Bcs1 AAA-ATPase suggests an airlock-like translocation mechanism for folded proteins. Nature Structural and Molecular Biology, 2020, 27, 142-149.	8.2	32
22	The Ccr4-Not complex monitors the translating ribosome for codon optimality. Science, 2020, 368, .	12.6	180
23	EDF1 coordinates cellular responses to ribosome collisions. ELife, 2020, 9, .	6.0	96
24	Structure and function of yeast Lso2 and human CCDC124 bound to hibernating ribosomes. , 2020, 18, e3000780.		0
25	Structure and function of yeast Lso2 and human CCDC124 bound to hibernating ribosomes. , 2020, 18, e3000780.		0
26	Structure and function of yeast Lso2 and human CCDC124 bound to hibernating ribosomes. , 2020, 18, e3000780.		0
27	Structure and function of yeast Lso2 and human CCDC124 bound to hibernating ribosomes. , 2020, 18, e3000780.		0
28	Spectrum and functional validation of PSMB5 mutations in multiple myeloma. Leukemia, 2019, 33, 447-456.	7.2	93
29	Thermophile 90S Pre-ribosome Structures Reveal the Reverse Order of Co-transcriptional 18S rRNA Subdomain Integration. Molecular Cell, 2019, 75, 1256-1269.e7.	9.7	48
30	Partially inserted nascent chain unzips the lateral gate of the Sec translocon. EMBO Reports, 2019, 20, e48191.	4.5	39
31	Structure and function of Vms1 and Arb1 in RQC and mitochondrial proteome homeostasis. Nature, 2019, 570, 538-542.	27.8	63
32	Structure of the 80S ribosome–Xrn1 nuclease complex. Nature Structural and Molecular Biology, 2019, 26, 275-280.	8.2	62
33	Ribosome–NatA architecture reveals that rRNA expansion segments coordinate N-terminal acetylation. Nature Structural and Molecular Biology, 2019, 26, 35-39.	8.2	79
34	Collided ribosomes form a unique structural interface to induce Hel2â€driven quality controlÂpathways. EMBO Journal, 2019, 38, .	7.8	232
35	Reconstitution of the human SRP system and quantitative and systematic analysis of its ribosome interactions. Nucleic Acids Research, 2019, 47, 3184-3196.	14.5	25
36	Structural and mutational analysis of the ribosome-arresting human XBP1u. ELife, 2019, 8, .	6.0	51

#	Article	IF	CITATIONS
37	Structural basis for coupling protein transport and N-glycosylation at the mammalian endoplasmic reticulum. Science, 2018, 360, 215-219.	12.6	177
38	Reconstitution of Isotopically Labeled Ribosomal Protein L29 in the 50S Large Ribosomal Subunit for Solution-State and Solid-State NMR. Methods in Molecular Biology, 2018, 1764, 87-100.	0.9	6
39	Folding pathway of an Ig domain is conserved on and off the ribosome. Proceedings of the National Academy of Sciences of the United States of America, 2018, 115, E11284-E11293.	7.1	86
40	BAX/BAK-Induced Apoptosis Results in Caspase-8-Dependent IL-1Î ² Maturation in Macrophages. Cell Reports, 2018, 25, 2354-2368.e5.	6.4	74
41	Suppressor mutations in Rpf2–Rrs1 or Rpl5 bypass the Cgr1 function for pre-ribosomal 5S RNP-rotation. Nature Communications, 2018, 9, 4094.	12.8	22
42	Structure of a hibernating 100S ribosome reveals an inactive conformation of the ribosomal protein S1. Nature Microbiology, 2018, 3, 1115-1121.	13.3	92
43	ALKBH5-induced demethylation of mono- and dimethylated adenosine. Chemical Communications, 2018, 54, 8591-8593.	4.1	31
44	Visualizing late states of human 40S ribosomal subunit maturation. Nature, 2018, 558, 249-253.	27.8	118
45	Cotranslational folding of spectrin domains via partially structured states. Nature Structural and Molecular Biology, 2017, 24, 221-225.	8.2	97
46	Structure of the <i>Bacillus subtilis</i> hibernating 100S ribosome reveals the basis for 70S dimerization. EMBO Journal, 2017, 36, 2061-2072.	7.8	74
47	Structural basis for ArfA–RF2-mediated translation termination on mRNAs lacking stop codons. Nature, 2017, 541, 546-549.	27.8	39
48	Structure of the 40S–ABCE1 post-splitting complex in ribosome recycling and translation initiation. Nature Structural and Molecular Biology, 2017, 24, 453-460.	8.2	77
49	Sucrose sensing through nascent peptideâ€meditated ribosome stalling at the stop codon of <i>Arabidopsis <scp>bZIP</scp>11 </i> <scp>uORF</scp> 2. FEBS Letters, 2017, 591, 1266-1277.	2.8	46
50	3.2-Ãresolution structure of the 90S preribosome before A1 pre-rRNA cleavage. Nature Structural and Molecular Biology, 2017, 24, 954-964.	8.2	95
51	Structural Basis for Polyproline-Mediated Ribosome Stalling and Rescue by the Translation Elongation Factor EF-P. Molecular Cell, 2017, 68, 515-527.e6.	9.7	118
52	An antimicrobial peptide that inhibits translation by trapping release factors on the ribosome. Nature Structural and Molecular Biology, 2017, 24, 752-757.	8.2	123
53	Ubiquitination of stalled ribosome triggers ribosome-associated quality control. Nature Communications, 2017, 8, 159.	12.8	249
54	Visualizing the Assembly Pathway of Nucleolar Pre-60S Ribosomes. Cell, 2017, 171, 1599-1610.e14.	28.9	162

#	Article	IF	CITATIONS
55	Preribosomes escaping from the nucleus are caught during translation by cytoplasmic quality control. Nature Structural and Molecular Biology, 2017, 24, 1107-1115.	8.2	35
56	Interdependent action of KH domain proteins Krr1 and Dim2 drive the 40S platform assembly. Nature Communications, 2017, 8, 2213.	12.8	38
57	The force-sensing peptide VemP employs extreme compaction and secondary structure formation to induce ribosomal stalling. ELife, 2017, 6, .	6.0	81
58	Cryo-EM structure of a late pre-40S ribosomal subunit from Saccharomyces cerevisiae. ELife, 2017, 6, .	6.0	77
59	Structural Dynamics of the YidC:Ribosome Complex during Membrane Protein Biogenesis. Cell Reports, 2016, 17, 2943-2954.	6.4	48
60	The cryo-EM structure of a ribosome–Ski2-Ski3-Ski8 helicase complex. Science, 2016, 354, 1431-1433.	12.6	108
61	A combined cryo-EM and molecular dynamics approach reveals the mechanism of ErmBL-mediated translation arrest. Nature Communications, 2016, 7, 12026.	12.8	103
62	The stringent factor RelA adopts an open conformation on the ribosome to stimulate ppGpp synthesis. Nucleic Acids Research, 2016, 44, 6471-6481.	14.5	129
63	Architecture of the 90S Pre-ribosome: A Structural View on the Birth of the Eukaryotic Ribosome. Cell, 2016, 166, 380-393.	28.9	184
64	Structure of the ribosome post-recycling complex probed by chemical cross-linking and mass spectrometry. Nature Communications, 2016, 7, 13248.	12.8	27
65	Ribosome-stalk biogenesis is coupled with recruitment of nuclear-export factor to the nascent 60S subunit. Nature Structural and Molecular Biology, 2016, 23, 1074-1082.	8.2	36
66	Structure of the hypusinylated eukaryotic translation factor eIF-5A bound to the ribosome. Nucleic Acids Research, 2016, 44, 1944-1951.	14.5	106
67	Small protein domains fold inside the ribosome exit tunnel. FEBS Letters, 2016, 590, 655-660.	2.8	69
68	Translation regulation via nascent polypeptide-mediated ribosome stalling. Current Opinion in Structural Biology, 2016, 37, 123-133.	5.7	137
69	Architecture of the Rix1–Rea1 checkpoint machinery during pre-60S-ribosome remodeling. Nature Structural and Molecular Biology, 2016, 23, 37-44.	8.2	104
70	Parallel Structural Evolution of Mitochondrial Ribosomes and OXPHOS Complexes. Genome Biology and Evolution, 2015, 7, 1235-1251.	2.5	77
71	Cryo-EM structure of the tetracycline resistance protein TetM in complex with a translating ribosome at 3.9-Ã resolution. Proceedings of the National Academy of Sciences of the United States of America, 2015, 112, 5401-5406.	7.1	58
72	Mitoribosome oddities. Science, 2015, 348, 288-289.	12.6	8

#	Article	IF	CITATIONS
73	Structure of a human translation termination complex. Nucleic Acids Research, 2015, 43, 8615-8626.	14.5	99
74	Role of the Cytosolic Loop C2 and the C Terminus of YidC in Ribosome Binding and Insertion Activity. Journal of Biological Chemistry, 2015, 290, 17250-17261.	3.4	29
75	Structure of the Bacillus subtilis 70S ribosome reveals the basis for species-specific stalling. Nature Communications, 2015, 6, 6941.	12.8	105
76	Structure of the native Sec61 protein-conducting channel. Nature Communications, 2015, 6, 8403.	12.8	169
77	Cotranslational Protein Folding inside the Ribosome Exit Tunnel. Cell Reports, 2015, 12, 1533-1540.	6.4	234
78	Translational arrest by a prokaryotic signal recognition particle is mediated by RNA interactions. Nature Structural and Molecular Biology, 2015, 22, 767-773.	8.2	29
79	ATP hydrolysis by the viral RNA sensor RIG-I prevents unintentional recognition of self-RNA. ELife, 2015, 4, .	6.0	75
80	Molecular Basis for the Ribosome Functioning as an L-Tryptophan Sensor. Cell Reports, 2014, 9, 469-475.	6.4	73
81	A new system for naming ribosomal proteins. Current Opinion in Structural Biology, 2014, 24, 165-169.	5.7	481
82	Structure of the mammalian oligosaccharyl-transferase complex in the native ER protein translocon. Nature Communications, 2014, 5, 3072.	12.8	127
83	Structures of the Sec61 complex engaged in nascent peptide translocation or membrane insertion. Nature, 2014, 506, 107-110.	27.8	186
84	Drug Sensing by the Ribosome Induces Translational Arrest via Active Site Perturbation. Molecular Cell, 2014, 56, 446-452.	9.7	104
85	A network of assembly factors is involved in remodeling rRNA elements during preribosome maturation. Journal of Cell Biology, 2014, 207, 481-498.	5.2	44
86	The <scp>C</scp> â€ŧerminal regions of <scp>YidC</scp> from <i><scp>R</scp>hodopirellula baltica</i> and <i><scp>O</scp>ceanicaulis alexandrii</i> bind to ribosomes and partially substitute for <scp>SRP</scp> receptor function in <i><scp>E</scp>scherichia coli</i> . Molecular Microbiology, 2014, 91, 408-421.	2.5	43
87	Molecular basis for erythromycin-dependent ribosome stalling during translation of the ErmBL leader peptide. Nature Communications, 2014, 5, 3501.	12.8	115
88	Cryoelectron Microscopic Structures of Eukaryotic Translation Termination Complexes Containing eRF1-eRF3 or eRF1-ABCE1. Cell Reports, 2014, 8, 59-65.	6.4	105
89	60S ribosome biogenesis requires rotation of the 5S ribonucleoprotein particle. Nature Communications, 2014, 5, 3491.	12.8	117
90	Visualization of a polytopic membrane protein during SecY-mediated membrane insertion. Nature Communications, 2014, 5, 4103.	12.8	60

#	Article	IF	CITATIONS
91	A structural model of the active ribosome-bound membrane protein insertase YidC. ELife, 2014, 3, e03035.	6.0	69
92	Structures of Nascent Polypeptide Chain-Dependent-Stalled Ribosome Complexes. , 2014, , 45-59.		1
93	Automatic post-picking using MAPPOS improves particle image detection from cryo-EM micrographs. Journal of Structural Biology, 2013, 182, 59-66.	2.8	26
94	Structural characterization of a eukaryotic chaperone—the ribosome-associated complex. Nature Structural and Molecular Biology, 2013, 20, 23-28.	8.2	79
95	Structures of the human and Drosophila 80S ribosome. Nature, 2013, 497, 80-85.	27.8	474
96	Promiscuous behaviour of archaeal ribosomal proteins: Implications for eukaryotic ribosome evolution. Nucleic Acids Research, 2013, 41, 1284-1293.	14.5	59
97	Structural basis of highly conserved ribosome recycling in eukaryotes and archaea. Nature, 2012, 482, 501-506.	27.8	210
98	Mechanisms of SecM-Mediated Stalling in the Ribosome. Biophysical Journal, 2012, 103, 331-341.	0.5	82
99	Structural view on recycling of archaeal and eukaryotic ribosomes after canonical termination and ribosome rescue. Current Opinion in Structural Biology, 2012, 22, 786-796.	5.7	37
100	Structure of the pre-60S ribosomal subunit with nuclear export factor Arx1 bound at the exit tunnel. Nature Structural and Molecular Biology, 2012, 19, 1234-1241.	8.2	103
101	Cryo-EM structure of the ribosome–SecYE complex in the membrane environment. Nature Structural and Molecular Biology, 2011, 18, 614-621.	8.2	264
102	Structure of the no-go mRNA decay complex Dom34–Hbs1 bound to a stalled 80S ribosome. Nature Structural and Molecular Biology, 2011, 18, 715-720.	8.2	150
103	The ribosomal tunnel as a functional environment for nascent polypeptide folding and translational stalling. Current Opinion in Structural Biology, 2011, 21, 274-282.	5.7	179
104	SecM-Stalled Ribosomes Adopt an Altered Geometry at the Peptidyl Transferase Center. PLoS Biology, 2011, 9, e1000581.	5.6	132
105	Signal sequence–independent SRP-SR complex formation at the membrane suggests an alternative targeting pathway within the SRP cycle. Molecular Biology of the Cell, 2011, 22, 2309-2323.	2.1	38
106	Localization of eukaryote-specific ribosomal proteins in a 5.5-â,,« cryo-EM map of the 80S eukaryotic ribosome. Proceedings of the National Academy of Sciences of the United States of America, 2010, 107, 19754-19759.	7.1	122
107	α-Helical nascent polypeptide chains visualized within distinct regions of the ribosomal exit tunnel. Nature Structural and Molecular Biology, 2010, 17, 313-317.	8.2	187
108	Mechanism of elF6-mediated Inhibition of Ribosomal Subunit Joining. Journal of Biological Chemistry, 2010, 285, 14848-14851.	3.4	107

#	Article	IF	CITATIONS
109	Cryo-EM structure and rRNA model of a translating eukaryotic 80S ribosome at 5.5-â,,« resolution. Proceedings of the National Academy of Sciences of the United States of America, 2010, 107, 19748-19753.	7.1	196
110	Structural Basis for Translational Stalling by Human Cytomegalovirus and Fungal Arginine Attenuator Peptide. Molecular Cell, 2010, 40, 138-146.	9.7	106
111	Structural Insight into Nascent Polypeptide Chain–Mediated Translational Stalling. Science, 2009, 326, 1412-1415.	12.6	263
112	Structure of Monomeric Yeast and Mammalian Sec61 Complexes Interacting with the Translating Ribosome. Science, 2009, 326, 1369-1373.	12.6	263
113	Signal Recognition Particle Receptor Exposes the Ribosomal Translocon Binding Site. Science, 2006, 312, 745-747.	12.6	133
114	Following the signal sequence from ribosomal tunnel exit to signal recognition particle. Nature, 2006, 444, 507-511.	27.8	184
115	Domain movements of elongation factor eEF2 and the eukaryotic 80S ribosome facilitate tRNA translocation. EMBO Journal, 2004, 23, 1008-1019.	7.8	373
116	SRP meets the ribosome. Nature Structural and Molecular Biology, 2004, 11, 1049-1053.	8.2	96
117	Structure of the signal recognition particle interacting with the elongation-arrested ribosome. Nature, 2004, 427, 808-814.	27.8	382
118	Structure of the 80S Ribosome from Saccharomyces cerevisiae—tRNA-Ribosome and Subunit-Subunit Interactions. Cell, 2001, 107, 373-386.	28.9	462
119	Architecture of the Protein-Conducting Channel Associated with the Translating 80S Ribosome. Cell, 2001, 107, 361-372.	28.9	368
120	Crystal structures of ribosome anti-association factor IF6. Nature Structural Biology, 2000, 7, 1156-1164.	9.7	70